Selective epitaxial growth of monolithically integrated GaN-based light emitting diodes with AlGaN/GaN driving transistors

Zhaojun Liu, Jun Ma, Tongde Huang, Chao Liu, and Kei May Lau

Selective epitaxial growth of monolithically integrated GaN-based light emitting diodes with AlGaN/GaN driving transistors

Zhaojun Liu,[a] Jun Ma,[a] Tongde Huang, Chao Liu, and Kei May Lau[b]
Photonics Technology Center, Department of Electronic and Computer Engineering,
Hong Kong University of Science and Technology, Clear Water Bay, Kowloon, Hong Kong

In this Letter, we report selective epitaxial growth of monolithically integrated GaN-based light emitting diodes (LEDs) with AlGaN/GaN high-electron-mobility transistor (HEMT) drivers. A comparison of two integration schemes, selective epitaxial removal (SER), and selective epitaxial growth (SEG) was made. We found the SER resulted in serious degradation of the underlying LEDs in a HEMT-on-LED structure due to damage of the p-GaN surface. The problem was circumvented using the SEG that avoided plasma etching and minimized device degradation. The integrated HEMT-LEDs by SEG exhibited comparable characteristics as unintegrated devices and emitted modulated blue light by gate biasing. © 2014 AIP Publishing LLC.
[http://dx.doi.org/10.1063/1.4867235]

There are growing interests in monolithic integration of GaN-based light emitting diodes (LEDs) and high-electron-mobility transistors (HEMTs) because of the demand of high luminous output large LEDs and HEMT's power handling capability.[1] Compared with conventional AC-DC power conversion using pulse width modulation (PWM) or analog current control using conventional silicon electronics, GaN-based power HEMTs have inherent advantages for LED drivers because of their superior properties such as high breakdown voltages, high operating frequencies, and wide operating temperature range.[2–4] Sharing the same GaN-based material platform, monolithic integration of LEDs and HEMTs can potentially reduce the form factor and manufacturing cost of an LED lighting system and greatly improve the system stability and reliability. Furthermore, monolithic integration will benefit other applications such as LED micro-displays and visible light communication (VLC).[5,6]

Despite these presumable advantages, limited results have been reported for the monolithic integration of GaN-based LEDs and HEMTs due to the complexity and complication of integration, including high-temperature epitaxial growth and device fabrication. There are three feasible approaches to integrate LEDs and HEMTs monolithically: selective epitaxial removal (SER), selective epitaxial growth (SEG), and flip-chip bonding (FCB). Each method has its pros and cons. FCB, typically performed with finished individual device structure, can minimize the integration-induced device degradation. However, associated processes for FCB, such as substrate thinning and polishing, complicate the overall fabrication process.[7] Recently, Li *et al.* and Kalaitzakis *et al.* reported monolithic integration of LEDs and HEMTs using the SER method, but obvious degradation in device performance resulting from the integration process was observed.[1,8]

In this work, we demonstrate the monolithic integration of high-performance GaN-based HEMTs and LEDs (HEMT-LED) by metal organic chemical vapor deposition

(MOCVD) selective epitaxial growth. We investigated the SER and SEG methods using a HEMT-on-LED structure. Minimized device degradation was achieved by the SEG process, and the integrated devices exhibited characteristics comparable to individual devices without integration. HEMT-LED devices emitted modulated blue light by gate-biasing of the HEMT part and illustrated potential applications of the integrated devices.

The HEMT structure was grown on commercial 2-inch LED wafers using an AIXTRON 2000HT MOCVD system. Trimethylgallium (TMGa), trimethylaluminum (TMAl), and ammonia (NH_3) were used as precursors for Ga, Al, and N, respectively. The HEMT structure consisted of, from bottom to top, 170 nm undoped GaN (u-GaN), 55 nm undoped $Al_{0.15}Ga_{0.85}N$, 200 nm u-GaN channel, 1 nm AlN spacer, and 20 nm undoped $Al_{0.30}Ga_{0.70}N$ barrier layers. Samples were grown and fabricated with SER (Fig. 1(a)) and SEG (Fig. 1(b)) methods separately. For sample A, the HEMT structure was grown on the LED wafer and then selectively removed using inductively coupled plasma (ICP) etching to expose the LED underneath. BCl_3 and Cl_2 were used for the ICP etching at a pressure of 5 mTorr. The coil power and platen power were 400 W and 80 W, respectively. As for sample B, the HEMT structure was selectively grown on the LED wafer using 1 μm SiO_2 as a pattern mask, which was removed by buffer oxide etchant (BOE) after the growth. A sample with identical HEMT structure and high-resistivity buffer was grown on sapphire as a reference. Material properties of the samples were characterized by room-temperature photoluminescence (PL) and van der Pauw Hall measurements. After the growth and material characterization, mesas of LEDs on samples A and B were created by ICP etching with the HEMT region protected by photoresist. Then mesas of HEMTs were created alternatively with the LED region protected by photoresist. Source/Drain ohmic contacts of the HEMTs were formed by e-beam evaporation of Ti/Al/Ni/Au and rapid thermal annealing (RTA) at 850 °C for 30 s in N_2. A Ni/Au current spreading layer (CSL) of the LEDs was then evaporated and subjected to 570 °C RTA for 5 min in an air atmosphere. Then Ti/Al/Ti/Au

---

[a]Z. Liu and J. Ma contributed equally to this work.
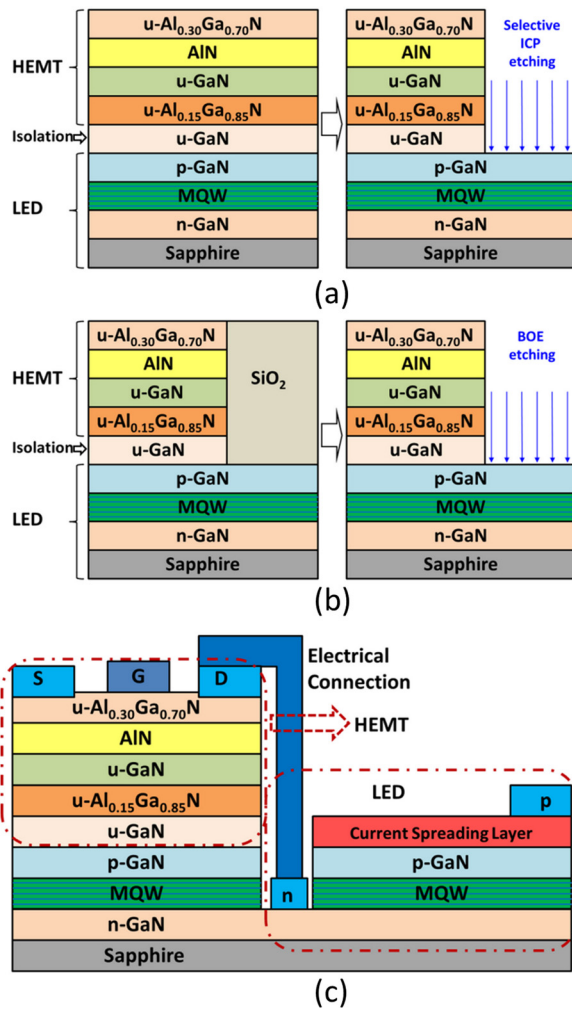[b]Email: eekmlau@ust.hk. Tel: (852)23587049. Fax: (852) 23581485

FIG. 1. Cross-sectional schematic of the (a) selective epi removal (SER), (b) selective epi growth (SEG) approaches, and (c) final structure of the HEMT-LED.
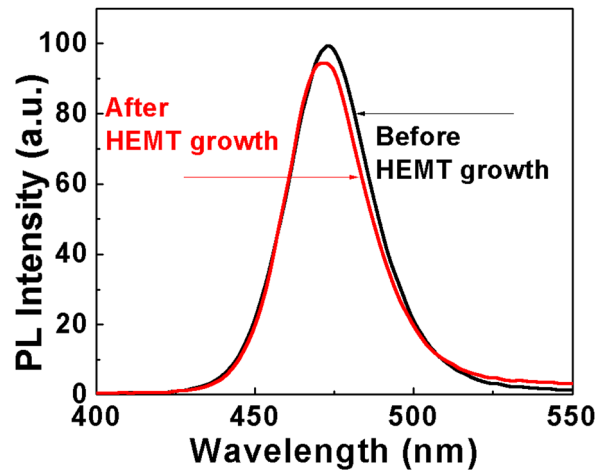

FIG. 2. PL spectra of the LED test sample before and after the simulated HEMT growth.

source injection). It can be seen that the PL peak intensity only decreased by about 5%. The PL FWHM before and after the simulated HEMT growth were comparable, indicating no significant degradation in optical properties and crystalline quality of the MQWs after the high temperature HEMT growth. The 2-D electron gas (2DEG) properties of the optimized HEMT structure were also monitored using room-temperature Hall measurements. The HEMT reference sample grown on sapphire exhibited a sheet resistance of 330 Ω/sq, with a mobility of 1470 cm^2/V·S and sheet carrier concentration of 1.26×10^{13} cm^{-2}, indicating good channel conductivity despite the somewhat lower growth temperature.

Figure 3 compares the transfer and output characteristics of the HEMTs fabricated on the reference sample, sample A

metal layers were evaporated as the p- and n-electrodes of the LED and patterned by lift-off process. Ni/Au gate metallization of the HEMTs was then realized. Outputs of the HEMTs were connected to the anodes of the LEDs by wire-bonding in this first generation of integrated devices.[9] The schematic cross-sectional view of the finished HEMT-LED is shown in Fig. 1(c).

Growth temperature was an important consideration for the HEMT growth on LED. Since InGaN/GaN multiple quantum wells (MQWs) are usually grown at a temperature much lower than that of AlGaN/GaN HEMTs (around 300 °C lower), there is a risk of degradation of the MQWs underneath during the HEMT growth, resulting in reduced PL intensity and widened full width at half maximum (FWHM) of the PL peak.[10] However, a conflicting choice of low growth temperature for the HEMTs might degrade the crystalline quality of the HEMT buffer layer and result in low mobility of the transistor. In this work, the growth temperature of the HEMTs was carefully optimized to be 1045 °C (100 °C lower than conventional growth in our system) to balance the considerations mentioned above. Fig. 2 shows the normalized PL spectra of an LED sample before and after a simulated HEMT growth in the MOCVD system (subjected to the same growth temperature without MO
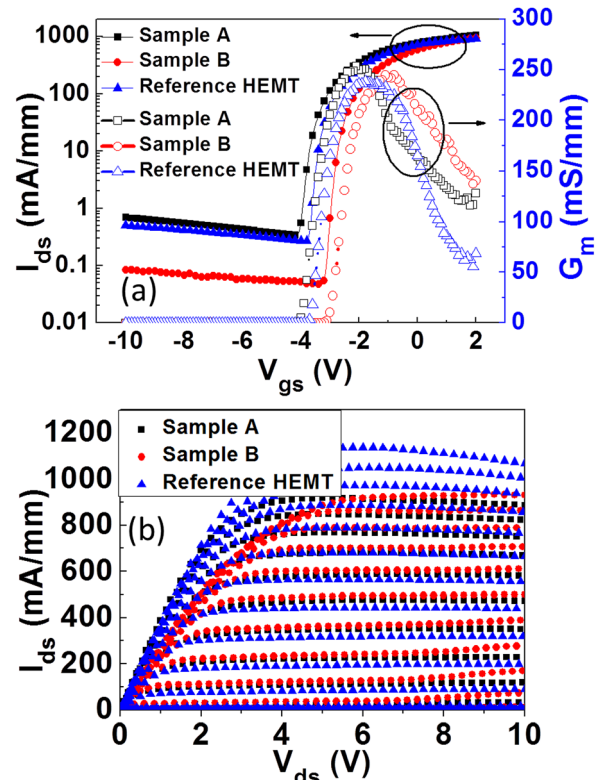

FIG. 3. (a) Transfer curves and (b) output curves of sample A (SER), sample B (SEG), and the reference HEMT.

TABLE I. Detailed device results of the reference HEMT, sample A, and sample B.

	Reference HEMT	Sample A (SER)	Sample B (SEG)
I_{on} (mA/mm)	1136	1038	940
I_{off} (mA/mm)	0.26	0.34	0.05
G_m (mS/mm)	238	253	245
R_{on} (ohm/mm)	2.84	2.58	3.58
V_{br} (V)	20.0	21.5	33.5

(by SER method), and sample B (by SEG method), respectively. Key device characteristics are listed in Table I. All three samples exhibited similar device characteristics. Peak extrinsic transconductance ($G_{m,max}$) was measured to be about 240 mS/mm at $V_{ds} = 6$ V. The I_{on} and I_{off} were around 1000 mA/mm and 0.3 mA/mm, respectively. This indicates that acceptable HEMT performance can be achieved with both SER and SEG technologies for monolithic integration. The I_{off} of the HEMT-LEDs was slightly larger than the typical value of GaN-based HEMTs due to the low growth temperature and the parasitic leakage path at the regrowth interface. Further investigation and optimization of the HEMT structure and growth techniques will be performed.

Compared with the SER method, the SEG method had significantly improved the LEDs' performance. I–V characteristics of the integrated LEDs are shown in Fig. 4. A reference LED sample was also fabricated to monitor the process. It was observed that sample A (by SER method) exhibited a forward voltage (V_F) of 17.1 V at 20 mA injection current, much larger than that of the reference sample ($V_F = 3.1$ V) and sample B (by SEG method, $V_F = 3.7$ V). The large V_F indicates that the LEDs are highly resistive leading to poor power efficiency.[11] Using the transmission line method (TLM), it was found that the V_F increase of sample A was mainly caused by a much higher p-type contact resistance. Ohmic p-type contacts were observed in both the reference sample and sample B. However, the p-type contact of sample A showed a Schottky contact behavior, and the contact resistance was large. For a better understanding of this phenomenon, X-ray Photoelectron Spectroscopy (XPS) was conducted, and the p-GaN valence band (E_V) edges of the three samples are plotted in Fig. 5. A band-bending potential
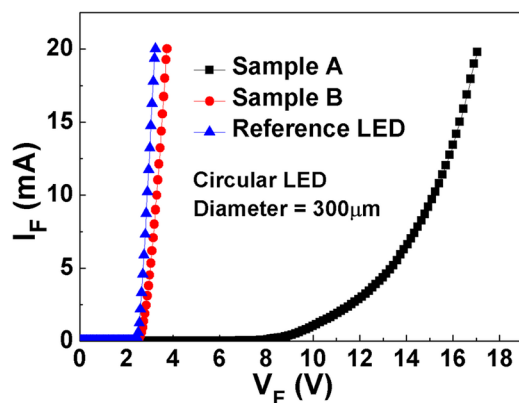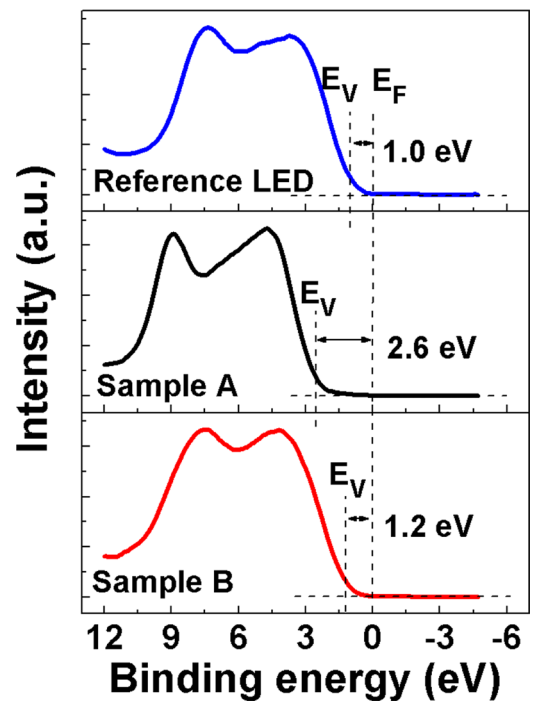

FIG. 5. P-GaN valence band edge of the reference LED, sample A (SER), and sample B (SEG) measured by XPS at a taking-off angle of 45°.

of about 1.0 eV was observed for the p-GaN of the reference sample, comparable to the reported values of 1.2–1.6 eV.[12] However, the band-bending potential of the p-GaN of sample A was about 2.6 eV, which is much larger than that of the reference sample. The increased potential was attributed to the plasma damage in the p-GaN surface of the LEDs. During the ICP etching, a nitrogen-deficient surface was produced due to the exposure of the p-GaN to the plasma, introducing donor states with concentrations above 1×10^{20} cm^{-3} in the surface layers.[13,14] These donor states can lead to a great reduction of the hole concentration, or even type conversion of the surface layers. Thus, the Schottky contact was observed for sample A. This plasma-damaged p-GaN can be one of the essential drawbacks of the SER method. Another drawback is the difficulty of locating the end point of the ICP etching precisely due to the negligible etching selectivity between undoped GaN and p-GaN. The V_F of LEDs will be greatly degraded in either under-etching or over-etching conditions. Considering the normal variation of MOCVD growth rate and ICP etching rate, it is difficult to have reproducible results with the SER method. However, similar problems were not encountered in using the SEG method, because the HEMT structure was selectively grown with the p-GaN protected by the SiO$_2$, and therefore, no ICP etching was needed. Comparing samples A and B, it can be seen that the band-bending potential was greatly reduced by 1.4 eV in the absence of plasma process. On the other hand, it is also noticed that the band-bending potential of sample B was 0.2 eV higher than that of the reference sample, indicating a slightly reduced hole concentration in the p-GaN. This can be explained by the H$_2$/NH$_3$ passivation of the p-type dopant during the HEMT growth.[15] Systematical investigation of the passivation and reactivation issues are underway.

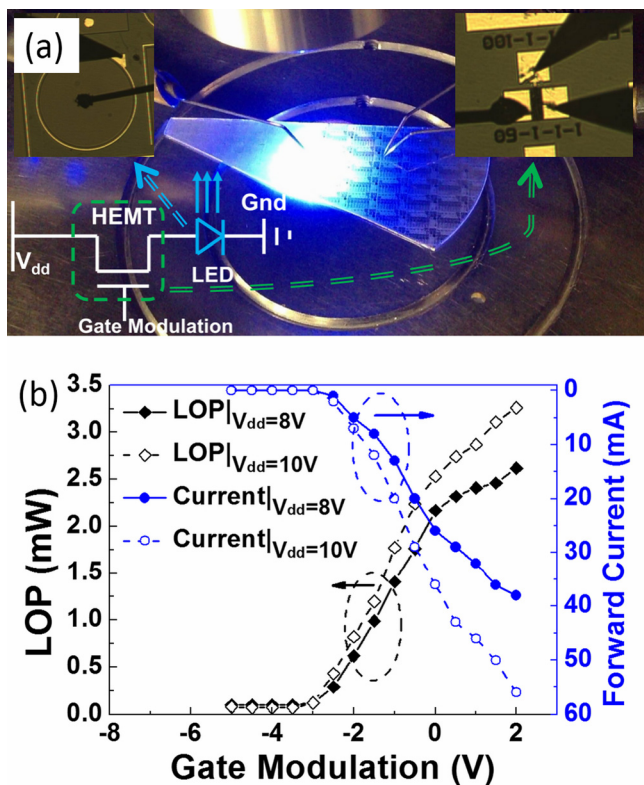FIG. 4. I–V characteristics of sample A (SER), sample B (SEG), and the reference LED.

FIG. 6. (a) The on-testing HEMT-LED emits blue light. The inset shows the circuit schematic of the device. (b) Light output power and I–V characteristics of the HEMT-LED with modulated gate biases and different V_{dd} voltages.

The HEMT-LED devices fabricated by the SEG method emitted modulated blue light at various gate biases, as shown in Fig. 6(a). We measured and plotted the corresponding forward current and light output power (LOP) against the applied bias (Fig. 6(b)), with the circuit diagram of the HEMT-LEDs shown in the inset of Fig. 6(a). The HEMT-LEDs showed gate controllability and driving capability, rendering this a suitable device for a wide range of applications, such as smart lighting, displays, and VLC. Besides the HEMT-on-LED structure reported in this work, another promising architecture for the monolithic integration of GaN HEMTs and LEDs is LED-on-HEMT. Both of the two architectures have their pros and cons. For example, the LED-on-HEMT structure is much easier to make on-chip interconnection between the cathode of the LED and the source/drain of the HEMT. But, it would be difficult to grow high performance LEDs on top of a HEMT epitaxial layer instead of a sapphire substrate. The HEMT-on-LED structure will not degrade the performance of the LED, but the interconnecting metal has to run the whole thickness of the LED plus the HEMT. The SER method leads to degradation of the LED p-contact when a HEMT-on-LED structure is used. However in a LED-on-HEMT structure, SER method could damage the AlGaN barrier layer and the 2DEG when the LED structure is selectively removed to expose the

HEMT underneath. To further boost the development of the monolithic integration of GaN HEMTs and LEDs, growth and fabrication techniques of both architectures need to be investigated for better device performance.

In conclusion, we have presented and compared monolithically integrated HEMT-LED devices fabricated by SER and SEG methods. The HEMT performance of both devices was comparable to the reference HEMTs on sapphire, but the LED performance was significantly improved by the SEG method. Much lower V_F was obtained across the LEDs compared with those fabricated with SER method due to the elimination of the ICP etching process. The HEMT-LED devices exhibited emission modulation capability and versatility for a broad range of applications.

[1]F. G. Kalaitzakis, E. Iliopoulos, G. Konstantinidis, and N. T. Pelekanos. Microelectron. Eng. **90**, 33 (2012).

[2]M. Araghchini, J. Chen, V. Doan-Nguyen, D. V. Harburg, D. Jin, J. Kim, M. S. Kim, S. Lim, B. Lu, D. Piedra, J. Z. Qiu, J. Ranson, M. Sun, X. H. Yu, H. Yun, M. G. Allen, J. A. del Alamo, G. DesGroseilliers, F. Herrault, J. H. Lang, C. G. Levey, C. B. Murray, D. Otten, T. Palacios, D. J. Perreault, and C. R. Sullivan, IEEE Trans. Power Electron. **28**, 4182 (2013).

[3]H. J. Chiu, Y. K. Lo, J. T. Chen, S. J. Cheng, C. Y. Lin, and S. C. Mou, IEEE Trans. Ind. Electron. **57**, 735 (2010).

[4]T. D. Huang, X. L. Zhu, and K. M. Lau, IEEE Electron Device Lett. **33**, 1123 (2012).

[5]Z. J. Liu, W. C. Chong, K. M. Wong, and K. M. Lau, J. Disp. Technol. **9**, 678 (2013).

[6]J. J. D. McKendry, D. Massoubre, S. Zhang, B. R. Rae, R. P. Green, E. Gu, R. K. Henderson, A. E. Kelly, and M. D. Dawson, J. Lightwave Technol. **30**, 61 (2012).

[7]Z. J. Liu, K. M. Wong, C. W. Keung, C. W. Tang, and K. M. Lau, IEEE J. Sel. Top. Quantum Electron. **15**, 1298 (2009).

[8]Z. Li, J. Waldron, T. Detchprohm, C. Wetzel, R. F. Karlicek, Jr., and T. P. Chow, Appl. Phys. Lett. **102**, 192107-1 (2013).

[9]Z. J. Liu, T. D. Huang, J. Ma, C. Liu, and K. M. Lau, IEEE Electron Device Lett. **35**, 330 (2014).

[10]C. J. Youn, T. S. Jeong, M. S. Han, J. W. Yang, K. Y. Lim, and H. W. Yu, J. Cryst. Growth **250**, 331 (2003).

[11]Y. Narukawa, M. Sano, M. Ichikawa, S. Minato, T. Sakamoto, T. Yamada, and T. Mukai, Jpn. J. Appl. Phys. **46**, L963 (2007).

[12]T. Hashizume, J. Appl. Phys. **94**, 431 (2003).

[13]X. A. Cao, S. J. Pearton, A. P. Zhang, G. T. Dang, F. Ren, R. J. Shul, L. Zhang, R. Hickman, and J. M. Van Hove, Appl. Phys. Lett. **75**, 2569 (1999).

[14]T. Narita, D. Kikuta, N. Takahashi, K. Kataoka, Y. Kimoto, T. Uesugi, T. Kachi, and M. Sugimoto, Phys. Status Solidi A **208**, 1541 (2011).

[15]S. Nakamura, N. Iwasa, M. Senoh, and T. Mukai, Jpn. J. Appl. Phys., Part 1 **31**, 1258 (1992).